Description of Scattering Object

A perfect electrically conducting (PEC) hexagonal prism with a circle-cylinder shaped duct.

Length Scale and Frequency Range

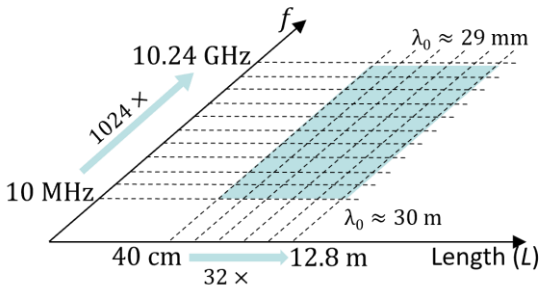

The problems of interest cover a range of 32x in physical length scale and 1024x in frequency; the ranges are logarithmically sampled to yield 66 scattering problems. Because the camera boxes are PEC, there are only 16+1 unique scattering problems in Problem Set IIISC. In these problems, the model sizes are in the range $0.013 \leq L/\lambda_0 \leq 438$, where λ_0 is the free-space wavelength.

Interesting Features

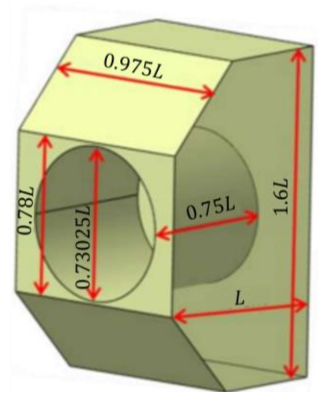

1. The camera box is designed as a host structure to enable reproducible RCS measurements of ducts. The flat-plate geometrical features of the housing promote strong backscattering in certain directions that are minimally affected by the scattering characteristics of any voids in the box [1],[2]. The camera box host structure used for Problem Sets IIISA and IIISB was modified in the following manner: its dimensions were scaled by 3× in the y-dimension and 2× in the z-dimension compared to that in [2] (see diagram for exact dimensions).
2. The sampling of the frequency range is distorted for this problem: scattering from the smallest camera box at frequencies $f \in$ {10, 20, 40, 80, 160, 320, 640, 1280, 2560, 5120, 7000, 10240} MHz are included in the problem set. This distortion is because of publicly available measurement data [1] and adds 1 unique scattering problem to the set.

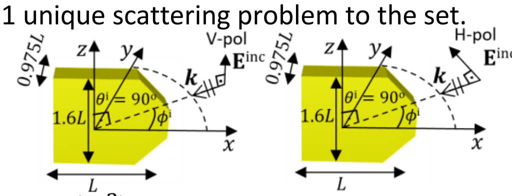

Quantities of Interest

Radar cross section (RCS) definition

$$\sigma_{vu}(\theta^{\mathrm{s}}, \phi^{\mathrm{s}}, \theta^{\mathrm{i}}, \phi^{\mathrm{i}}) = \lim_{R\to\infty} 4\pi R \frac{|\hat{v}(\theta^{\mathrm{s}}, \phi^{\mathrm{s}}) \cdot \mathbf{E}^{\mathrm{scat}}(\theta^{\mathrm{s}}, \phi^{\mathrm{s}})|^2}{|\hat{u}(\theta^{\mathrm{i}}, \phi^{\mathrm{i}}) \cdot \mathbf{E}^{\mathrm{scat}}(\theta^{\mathrm{i}}, \phi^{\mathrm{i}})|^2} \quad : \text{ RCS } (\mathrm{m}^2)$$

$$\sigma_{vu,\mathrm{dB}}(\theta^{\mathrm{s}}, \phi^{\mathrm{s}}, \theta^{\mathrm{i}}, \phi^{\mathrm{i}}) = 10 \log_{10} \sigma_{vu} \quad : \text{RCS in dB (dBsm)}$$

$$\sigma_{vu,\mathrm{dB}}^{TH}(\theta^{\mathrm{s}}, \phi^{\mathrm{s}}, \theta^{\mathrm{i}}, \phi^{\mathrm{i}}) = \max\left(\sigma_{vu,\mathrm{dB}}, TH_{vu,\mathrm{dB}}\right) - TH_{vu,\mathrm{dB}} \quad : \text{Thresholded RCS}$$

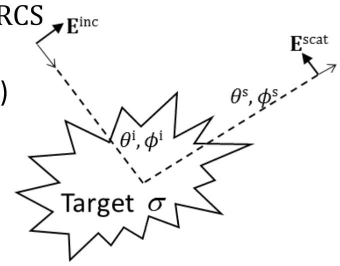

1. Set $\theta^{\mathrm{i}} = 90^{\mathrm{o}}$. Vary $0^{\mathrm{o}} \leq \phi^{\mathrm{i}} \leq 180^{\mathrm{o}}$ (every 0.5° in the interval).
2. Compute back-scattered $\sigma_{\theta\theta,\mathrm{dB}}$ and $\sigma_{\phi\phi,\mathrm{dB}}$ (the VV- and HH-pol RCS in dB) at $N_\phi = 361$ scattering directions.

Performance Measures

Error Measure: Simulation errors shall be quantified using

$$avg.err_{uu,\mathrm{dB}}^{TH} = \frac{1}{2\pi}\int_0^{2\pi} \left|\sigma_{uu,\mathrm{dB}}^{TH}(\phi^s) - \sigma_{uu,\mathrm{dB}}^{\mathrm{ref},TH}(\phi^s)\right| d\phi^s \approx \frac{1}{N_\phi}\sum_{n=1}^{N_\phi}\left|\sigma_{uu,\mathrm{dB}}^{TH}(\phi_n^{\mathrm{s}}) - \sigma_{uu,\mathrm{dB}}^{\mathrm{ref},TH}(\phi_n^{\mathrm{s}})\right| \text{ (dB) for } u \in \{\theta, \phi\}$$

where

$$TH_{uu,\mathrm{dB}} = \max_{\phi^s} \sigma_{uu,\mathrm{dB}}^{\mathrm{ref}} - 80 \text{ (dB)}$$

This error measure discounts errors in RCS values smaller than TH.

Cost Measure: Simulation costs shall be quantified using observed wall-clock time and peak memory/process

$$t^{\mathrm{wall}}\text{(s) and } mem^{\mathrm{maxproc}}\text{(bytes)}$$

as well as the "serialized" CPU time and total memory requirement

$$t^{\text{total}} = N_{\text{proc}} \times t^{\text{wall}}\text{(s) and } mem^{\max} = N_{\text{proc}} \times mem^{\text{maxproc}} \text{ (bytes)}$$

Here, N_{proc} denotes the number of processes used in a parallel simulation. It is expected that results will be reported for at least 2 runs: "Efficient" (small N_{proc}) and "Fast" (large N_{proc}).

Study 1: Error vs. Cost Sweep

Fix frequency and fix camera box dimensions. Simulate many error levels (proxy: mesh densities) for 4 cases:

Case 1: *f*=10 MHz, *L*=40 cm Case 2: *f*=7 GHz, *L*=40 cm

Case 3: *f*=10 MHz, *L*=6.4 m Case 4: *f*=320 MHz, *L*=6.4 m

It's recommended to simulate as many error levels (mesh densities) as possible. 3-5 error levels is typical. A typical error-vs.-cost study will consist of 4x3-5=12-20 simulations.

Study 2: Frequency Sweep

Fix camera box dimensions and error level (proxy: mesh density). Simulate many frequencies for 4 cases:

Case 1: *L*=40 cm, error level 1 (coarsest mesh) Case 2: *L*=6.4 m, error level 1 (coarsest mesh)

Case 3: *L*=40 cm, error level 2 (finer mesh) Case 4: *L*=6.4 m, error level 2 (finer mesh)

Frequencies shall be chosen as $f \in \{10, 20, 40, \ldots, 5120, 10240\}$ MHz. It's recommended to simulate as many frequencies as possible. A full frequency-sweep study will consist of 4x11=44 simulations.

Study 3: Size Sweep

Fix frequency and error level (proxy: mesh density). Simulate many sizes for 4 cases:

Case 1: *f*=10 MHz, error level 1 (coarsest mesh) Case 2: *f*=320 MHz, error level 1 (coarsest mesh)

Case 3: *f*=10 MHz, error level 2 (finer mesh) Case 4: *f*=320 MHz, error level 2 (finer mesh)

Dimensions shall be chosen as $L \in \{40, 80, 120, \ldots, 640, 1280\}$ cm. It's recommended to simulate as many sizes as possible. A full size-sweep study will consist of 4x7=28 simulations.

Reference Quantities of Interest

The following RCS data are made available in the benchmark to enable participants to calibrate their simulators:

8 RCS measurement results corresponding to the smallest cylindrical-duct camera box (*L*=40 cm) at frequencies $f \in \{2560, 5120, 7000, 10240\}$ MHz. These data are provided for ϕ^{i} sampled every 0.5°.

4 RCS simulation results for the smallest cylindrical-duct camera box at the above 4 frequencies found by using the ARCHIE-AIM code, a frequency-domain FFT-accelerated integral-equation solver developed at UT Austin [3]-[5].

References

[1] J. T. Kelley *et al*., "Reproducible measurements of "fan blades in a pipe" CEM benchmark," in *Proc. Antenna Meas. Techn. Assoc. Symp.,* Oct. 2023.

[2] A. E. Yilmaz *et al*., "Camera boxes: a set of complex scattering problems to test EM simulations and measurements," in *Proc. IEEE Antennas Propag. Soc. Int. Symp.*, July 2022.

[3] M. F. Wu, G. Kaur, and A. E. Yılmaz, "A multiple-grid adaptive integral method for multi-region problems," *IEEE Trans. Antennas Propag.*, vol. 58, no. 5, pp. 1601-1613, May 2010.

[4] F. Wei and A. E. Yılmaz, "A more scalable and efficient parallelization of the adaptive integral method part I: algorithm," *IEEE Trans. Antennas Propag.*, vol. 62, no.2, pp. 714-726, Feb. 2014.

[5] J. W. Massey, V. Subramanian, C. Liu, and A. E. Yılmaz, "Analyzing UHF band antennas near humans with a fast integral-equation method," in *Proc. EUCAP*, Apr. 2016.